Journal of Volcanology and Geothermal Research 282 (2014) 92–102

Contents lists available at ScienceDirect

Journal of Volcanology and Geothermal Research

journal homepage: www.elsevier.com/locate/jvolgeores

Emplacement and erosive effects of lava in south Kasei Valles, Mars

Colin M. Dundas *, Laszlo P. Keszthelyi

Astrogeology Science Center, U.S. Geological Survey, 2255 N. Gemini Dr., Flagstaff, AZ 86001, USA

ARTICLE INFO

Article history:
Received 17 January 2014
Accepted 2 June 2014
Available online 20 June 2014

Keywords:
Flood lavas
Outflow channels
Lava erosion
Mars

ABSTRACT

Although it has generally been accepted that the Martian outflow channels were carved by floods of water, observations of large channels on Venus and Mercury demonstrate that lava flows can cause substantial erosion. Recent observations of large lava flows within outflow channels on Mars have revived discussion of the hypothesis that the Martian channels are also produced by lava. An excellent example is found in south Kasei Valles (SKV), where the most recent major event was emplacement of a large lava flow. Calculations using high-resolution Digital Terrain Models (DTMs) demonstrate that this flow was locally turbulent, similar to a previously described flood lava flow in Athabasca Valles. The modeled peak local flux of approximately 10^6 m^3 s^{-1} was approximately an order of magnitude lower than that in Athabasca, which may be due to distance from the vent. Fluxes close to 10^7 m^3 s^{-1} are estimated in some reaches but these values are probably records of local surges caused by a dam-breach event within the flow. The SKV lava was locally erosive and likely caused significant (kilometer-scale) headwall retreat at several cataracts with tens to hundreds of meters of relief. However, in other places the net effect of the flow was unambiguously aggradational, and these are more representative of most of the flow. The larger outflow channels have lengths of thousands of kilometers and incision of a kilometer or more. Therefore, lava flows comparable to the SKV flow did not carve the major Martian outflow channels, although the SKV flow was among the largest and highest-flux lava flows known in the Solar System.
Published by Elsevier B.V.

1. Introduction

Flood lavas cover a large fraction of the Martian surface and make up much of the volume of the crust (Greeley and Schneid, 1991; McEwen et al., 1999; Keszthelyi and McEwen, 2007; Caudill et al., 2012). However, the emplacement dynamics of a Martian flood lava flow have only been detailed in one case, the Athabasca Valles lava (Jaeger et al., 2007, 2010). Parts of the Athabasca Valles lava exhibit type examples of "platy-ridged" morphology, which corresponds to rubbly pahoehoe on Earth (Keszthelyi et al., 2000, 2004). The flow started from the Cerberus Fossae fissures, draped the entire surface of the ~300-km-long Athabasca Valles outflow channel with a few meters of lava that were left behind as the flow waned, filled and overflowed the Cerberus Palus basin, and reached a maximum distance of 1400 km from the source (Jaeger et al., 2007, 2010). A remarkable feature about this flow is that calculations indicate that it was emplaced turbulently with a very high peak volumetric flux around 10^7 m^3 s^{-1} (Jaeger et al., 2010). Although it was once thought that flood lavas on Earth were emplaced in this manner (e.g., Shaw and Swanson, 1970; Swanson et al., 1975), subsequent work concluded that this mechanism is not observed in terrestrial lavas (e.g., Self et al., 1996, 1997, 1998; Keszthelyi et al., 2006). Instead, flood lavas on Earth are usually emplaced over decadal timescales as inflating sheet flows with average fluxes of order 10^3–10^4 m^3 s^{-1}.

The rapid, turbulent emplacement of the Athabasca Valles flow, and its close fit within the outflow channel, left Jaeger et al. (2010) unable to rule out the possibility that the lava eroded the channel. Erosion by lava was considered and dismissed as the general explanation for large Martian outflow channels in early studies on the basis that catastrophic water floods best explained the observed assemblage of landforms (e.g., Carr, 1974; Baker, 1982). Baker (1982) specifically noted the lack of scabland erosion, absence of large deposits at channel mouths, high width/depth ratios and occurrence of headcuts as inconsistent with lava erosion. Subsequently, large channels, unambiguously carved by lava, have been described on Venus (e.g., Baker et al., 1992) and Mercury (Head et al., 2011; Hurwitz et al., 2013a), in addition to the previously-known sinuous rilles on the Moon (e.g., Hurwitz et al., 2013b, and references therein). Coupled with the observations of Athabasca Valles by Jaeger et al. (2010), these features have revived consideration of the volcanic hypothesis for Martian outflow channels (e.g., Leverington, 2004, 2007, 2009, 2011; Hurwitz and Head, 2012; Leone, 2014). However, Athabasca Valles is not an ideal setting to investigate erosion by lava because the flow almost perfectly matches the channel capacity, which makes it hard to determine how the lava interacted with the pre-eruption surface. Detailed studies on Venus and Mercury are difficult because they lack high-resolution data.

* Corresponding author.
E-mail address: cdundas@usgs.gov (C.M. Dundas).

http://dx.doi.org/10.1016/j.jvolgeores.2014.06.005
0377-0273/Published by Elsevier B.V.

Kasei Valles is the largest of the Martian outflow channels, extending more than 3000 km from a source in Echus Chasma. Like Athabasca Valles, it hosts well-preserved platy-ridged lava suggestive of a high-flux flow, which led us to consider it for this study. Because Kasei Valles is up to several kilometers deep, the lava flow is confined near the bottom of the channel, unlike Athabasca Valles where lava completely filled the decameters-deep channel. This makes it easier to understand topographic interactions and detect erosion by lava, since the pre-existing surface can be better understood. Although the Kasei Valles flow is not as exquisitely preserved as that in Athabasca, it is an excellent target for investigating erosion by lava on Mars.

2. Methods

The focus of this paper is on the emplacement and erosive effects of the most recent lava in south Kasei Valles (SKV). Key input parameters are extracted from Digital Terrain Models (DTMs) derived from images from the Mars Reconnaissance Orbiter Context Camera (CTX; Malin et al., 2007). Production methods for such DTMs are similar to those used for the High Resolution Imaging Science Experiment (HiRISE; Kirk et al., 2008), utilizing a combination of the USGS Integrated Software for Imagers and Spectrometers (ISIS) and BAE Systems SOCET Set software. CTX DTMs can have pixel scales as small as 20–25 m, but some DTMs were extracted at lower resolution. The vertical precision of stereo DTMs is typically close to one image pixel. DTMs are controlled with data from the Mars Orbiter Laser Altimeter (MOLA), so errors in slope over baselines longer than MOLA resolution should be small. Measurements of elevations and profiles were made using the ESRI ArcGIS software.

We estimate lava fluxes using standard equations for turbulent flow through a channel (e.g., Shaw and Swanson, 1970; Keszthelyi and Self, 1998; Keszthelyi et al., 2006; Jaeger et al., 2010). The mean flow velocity $\langle v \rangle$ is given by

$$\langle v \rangle = (\mathrm{gd}\sin(\theta)/\mathrm{C_f})^{1/2} \quad (1)$$

$$Cf = (1/32)\left(\log_{10}(6.15(2Re + 800)/41)^{0.92}\right)^{-2} \quad (2)$$

$$Re = \rho d\langle v \rangle/\eta \quad (3)$$

where C_f is a friction factor (Goncharov, 1964) and Re is the Reynolds number. Input parameters are discussed below. In this formulation, C_f must be determined recursively. These expressions were derived for mildly turbulent flow (Re of 500–10,000), but may be used for higher values (at least ~10^5) with some caution (e.g., Keszthelyi and Self, 1998; Jaeger et al., 2010). A Newtonian lava flow emplaced in the laminar regime has velocity given by the Jeffreys equation (Jeffreys, 1925):

$$\langle v \rangle = \rho g \sin(\theta) d^2/3\eta. \quad (4)$$

This equation is used if the Reynolds number is less than 500. The constant 3 is appropriate for a broad shallow channel and translating crust (used here), but a value of 8 would be used for a filled lava tube, and 12 for a sheet flow with a stationary crust (e.g., Bird et al., 1960). Although the final preserved crust may have been stationary, we consider a translating crust to be the more likely scenario near peak flux. Most of the scenarios considered in this paper are turbulent and use Eqs. (1)–(3). We note that many studies of lava flow emplacement assume a Bingham plastic rheology for lava to crudely approximate the effect of the crust on a lava flow. However, for a deep, high-velocity flow near peak discharge, the effect of the crust should be minor and a simple Newtonian rheology should be adequate. The local volumetric flux Q for a rectangular channel is given by

$$Q = Wd\langle v \rangle, \quad (5)$$

the volume of lava flowing past the cross-section location per unit time.

In principle, these equations could be used to examine any stage of the flow, given the flow depth and channel shape at that time. However, the DTMs show only the high-lava mark and the final channel shape. (Occasionally multiple marks indicate stages in the flow, but we consider only the highest lava level.) We can estimate the peak lava flux at a point using these two observations, if we assume that lava drained from the channel (as in Athabasca Valles) and that erosion of the channel after the high-lava mark was set was minimal. At each of the sites we examine, the first assumption is reasonable since the lava appears to be only a thin coating on the surface. The validity of the second assumption is discussed on a site-by-site basis below. Note that this method gives the peak value of the local, instantaneous flux, which is not identical to the effusion rate at the vent. (See Harris et al. (2007) for a discussion of eruption rate terminology.) In most cases, peak flux will be less than peak effusion rate and diminish away from the vent, because brief high values of the lava flux will be attenuated downstream (e.g., by branching and basin-filling).

Parameters needed for these equations include gravity g, flow depth d, flow width W, slope θ, lava density ρ, and viscosity η. Real cross-sections may deviate significantly from rectangular channels, so for d we use hydraulic radius, equal to the cross-sectional area divided by the wetted perimeter (Shaw and Swanson, 1970). Slopes were estimated by measuring the elevation offset between high-lava marks a few km upstream and downstream from measured cross-sections, with a horizontal distance measured parallel to the flow direction, which should approximate the lava surface slope at peak flow. The specific measurement points were chosen at locations where the flow edge was well-defined. The few-km baseline was chosen to reduce errors due to surface roughness while still capturing a value close to the local slope; however, few-meter-scale roughness (including the relief of the flow edge) and the relatively coarse resolution of the DTMs may introduce some error. Additionally, some high-lava marks may reflect run-up of the flow onto obstacles, so opposite banks of the flow are not always at precisely the same level. To minimize these effects, we averaged 2–3 separate slope measurements with distinct (but nearby) endpoints for each cross-section. These measurements show significant scatter at each cross-section, resulting in similarly significant uncertainty in the lava flux. This scatter represents not only error in the DTMs but also different measurement baselines and locations. In the worst case the extreme is within 60% of the mean. This is non-trivial, but our conclusions are impervious to this level of uncertainty and the variations assumed for the other parameters.

Since we do not have strong constraints on the SKV lava composition, we examine viscosities of 10, 100 and 1000 Pa s and densities of 1400, 2300 and 2900 kg m^{-3}. These viscosity values (after Keszthelyi et al., 2000) are reasonable for flows ranging from komatiites through basalts to basaltic andesites. Given the generally basaltic nature of Mars (e.g., McSween et al., 2009), the lower viscosities are preferred. We note that Mangold et al. (2010) observed a basaltic mineralogy for possibly-associated lava in Echus Chasma. Jaeger et al. (2010) considered viscosities of 10, 50 and 100 Pa s and densities of 850, 1400 and 2300 kg m^{-3} in modeling the Athabasca Valles flow. We replaced their lowest density with a higher value since vesicularities of ~70% are probably only a near-vent phenomenon (e.g., Swanson, 1973), while far from the vent the lava may be substantially degassed. For comparison, Alberti et al. (2012) estimated porosities of 40–50% within a few hundred km of the source of the Athabasca Valles lava by examining the dielectric properties. Although they considered this porosity inconsistent with lava, it is consistent with vesicular basalt and the brecciated crusts described by Keszthelyi et al. (2004), and would give bulk

densities similar to those used above. As will be seen, although the model outputs vary widely within this parameter space, the variation is not enough to affect our conclusions.

3. Observations

3.1. The south Kasei Valles lava

Fig. 1A gives an overview of the lava in SKV. Platy-ridged lava extends north and east from a plain and travels approximately 1400 km down SKV. The location of the vent is not certain, but it is likely that the distance from the vent to the toe of the flow is at least several hundred km greater. In this study we only consider the lava within SKV, but potentially associated platy-ridged lava is found in north Kasei Valles (NKV), the Sacra Sulci region, and Echus Chasma (Chapman et al., 2010). About 200 km from the plain in the southwestern part of Fig. 1A, the flow goes over a lava fall at the upper cataract and then passes through a series of constrictions from landslides or impinging fans of wall material (Fig. 1B). Locally, the width and slope are highly variable due to interactions with complex topography, but over the last ~950 km the flow is mostly 5–20 km wide and occupies the floor of a nearly straight valley. Over this stretch the average slope is ~0.05°, but only ~0.03° if the vicinity of the lower cataract is excluded. For comparison, typical slopes are ~5° for shield volcanoes, ~0.05° for terrestrial flood lavas, and 0.02–0.03° for Athabasca Valles. We have not mapped the flow in detail, but the area is $>10^4$ km^2, suggesting a lava volume of hundreds of km^3 if the average depth was tens of meters. Both the length and area are lower bounds since these dimensions only apply to lava in SKV, but are very typical of flood lavas on Earth (e.g., Keszthelyi et al., 2006).

Chapman et al. (2010) proposed that the platy unit in Kasei Valles was emplaced as a series of flows over ~150 Myr with a mean age of ~200 Ma. However, the ages presented in Chapman et al. (2010) have the most distal material as the youngest, which is not consistent with expectations based on the law of superposition—younger flows should also have buried proximal surfaces. There are significant uncertainties in dating young surfaces on Mars, so we are more confident in the relative ages derived from superposition than from crater counting. The unit we investigated in SKV seems to have been emplaced in a single brief geologic event. We have not observed any definite flow fronts within the lava in SKV, despite the well-preserved flow surface. The handful of candidate fronts within the flow are consistent with locally inflated lobes rather than separate flows, or with late breakouts from the flow interior. Other possible boundaries appear to be textural differences within a single flow. However, the flow has not been mapped in detail and, as discussed in Section 4.1, it is possible that one or more of the candidate fronts will be found to be a real boundary.

3.2. Local analyses

We examined four CTX DTMs at locations indicated in Fig. 1 (Table 1). The first covers the upper cataract, the second covers constriction 3, the third covers a typical reach of the channel below the constrictions, and the fourth covers the lower cataract. These sites have important topographic interactions and are locations where much of the lava drained away, allowing measurements of topographic profiles that approximate the original surface. In the first DTM, we studied flow through a single cross-section to obtain an estimate of the peak lava flux entering SKV. In the second, we examined three cross-sections above and within the channel of constriction 3, allowing comparison of results for several locations in close proximity. The third DTM was not used for flux measurements, but demonstrates that the overall effect of the lava was aggradational along most of Kasei Valles. In the final DTM, we again examined a single cross-section to understand the distal lava flux. The cross-sections are illustrated in Figs. 2–3, and topographic data are given in Table 2.

The first CTX DTM covers the region between the upper cataract and constriction 1 (Fig. 2A–B). We made a flux estimate at cross-section A–A′ (Fig. 3), just above the upper cataract (see Fig. 1B). A small amount of lava drained through a side channel before rejoining the main flow and

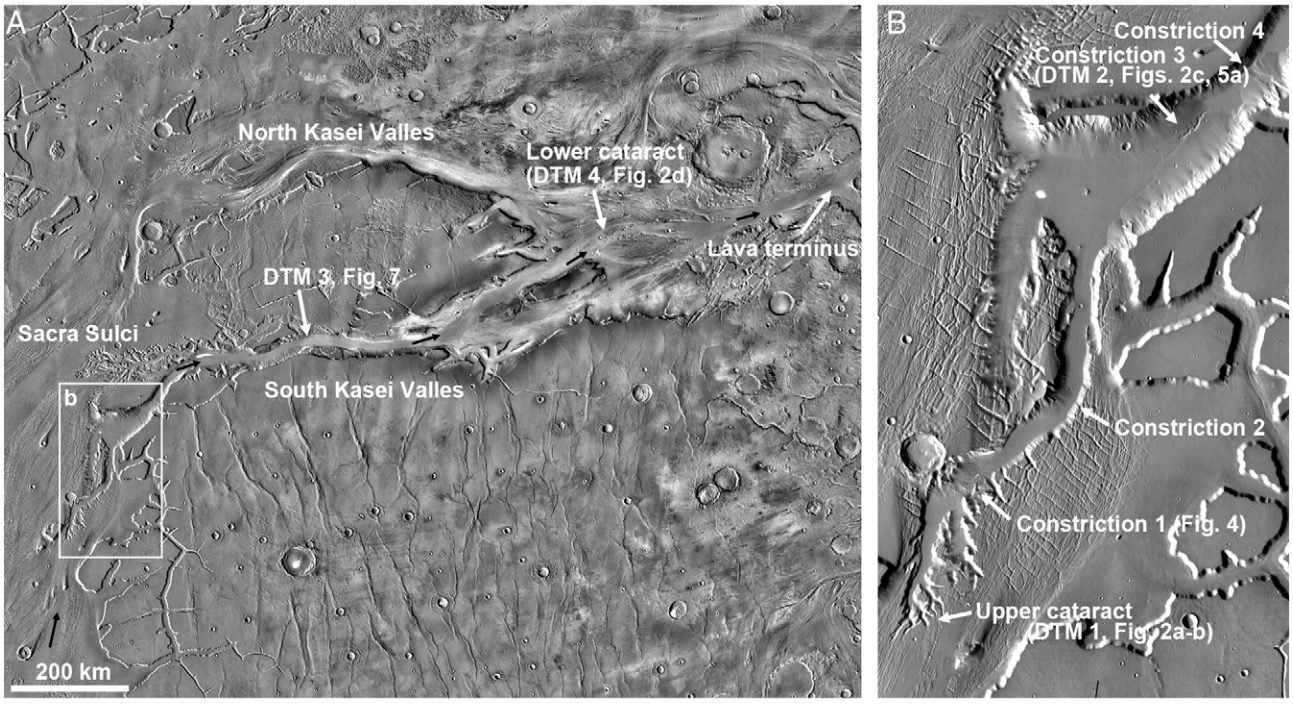

Fig. 1. A) Overview of the Kasei Valles region (roughly 14–30°N, 284–304°E). The south Kasei Valles lava separates from a body of platy-ridged lava at lower left. Black arrows indicate the primary path of the SKV lava. The lava corresponds to the relatively smooth, flat central channel floor. B) Detail of the upper cataract and four constrictions discussed in the text, numbered 1–4. Constrictions 3 and 4 were described by Williams and Malin (2004). Image in both panels is from the Thermal Emission Imaging System (THEMIS; Christensen et al., 2004) Daytime infrared global mosaic in simple cylindrical projection (credit: NASA/THEMIS Team/Arizona State University). North is up and illumination from the left in all figures in this paper.

Table 1
CTX DTM source images.

DTM	CTX images
1	B09_013152_1984_XN_18N074W
	B09_013297_1984_XN_18N074W
2	P03_002287_2005_XI_20N072W
	P05_002788_2005_XI_20N072W
3	G15_024215_2048_XN_24N069W
	G16_024637_2048_XN_24N069W
4	P05_002814_2051_XI_25N061W
	P06_003513_2057_XI_25N061W

is missed by this cross-section, but this should be a minor source of uncertainty. Even after examining the full range of reasonable input parameters, the lava flux varies only between 2×10^5 and 10^6 m^3 s^{-1} (Table 3). Flow was turbulent for values appropriate for mafic–ultramafic flows but would have been laminar for intermediate (i.e., basaltic-andesite) compositions.

There is evidence for limited erosion by lava at the main lava falls. The images show that some lava reached northward past the main lava falls (Fig. 2B). However, the current topography would likely have captured the flow and prevented it passing to the north of the cataract. To provide a surface that the lava could traverse, it is likely that the pre-lava cataract was cut back by roughly 1 km. The talus-covered amphitheater that captured the lava drops 500 m over about 1 km horizontal distance, a situation highly conducive to mechanical erosion. It is unlikely that the cataract retreated more than 1–2 km, because the initial position of the scarp must have enabled it to capture a large fraction of the flow and drive subsequent erosion. Supporting the interpretation of local erosion by lava, the section of the cataract below the lava falls is wider and deeper than the other arms (Fig. 2A–B). An incised inner channel spanned by A–A′ feeds into the cataract head. It is likely that this was carved by the SKV flow as well, since the floor of the channel lies as much as tens of meters below the presumed downstream continuation on the far side of the cataract. This implies that our estimated lava flux here is an upper limit. However, it is probably not much above the peak since the inner channel only accounts for about 20% of the cross-sectional area and could have been partly eroded before the high-lava mark was established.

Over a distance of about 40 km between the cataract and constriction 1, the high-lava marks are essentially level and were established while lava was deeply ponded. The deflated flow surface shows that the lava depth was >200 m. The surface slope was so low that we do not consider flux estimates reasonable in this region, since very small absolute errors in the DTM would have a dramatic effect on flux estimates. The flat floor of the channel here suggests that the net effect of the lava was to bury rather than erode the surface.

Constriction 1 (Fig. 4) is marked by a cataract that has evidently eroded headward through the blocking material. Downstream, the flow passes through constriction 2 and then opens into a broad depression. High-lava marks demonstrate that lava was significantly deeper here at the peak of the flow and subsequently drained through the third constriction, but high-resolution topography of the cataract is not available for more detailed analyses.

The second DTM (Fig. 2C) covers constriction 3. Cross-section B–B′ is several km upstream from the channel head, C–C′ is only a short distance upstream, and D–D′ is a cross-section of the inner channel. Examining multiple profiles lets us test internal consistency and better understand the importance of erosion. The channel ran approximately bank-full at each of these profiles, because we measure from the high-lava mark for the first two and the lava overflowed the channel a short distance downstream from the third. At B–B′ and C–C′, the lava has built up the original surface (Fig. 5), so we estimated the original topography by excising the platy-ridged surface from the DTM. We performed local polynomial interpolations in ArcMap using points from the north and south of the channel separately to extrapolate slopes, using a basis function elongated in the down-slope direction and fitting second-order polynomials. The gap in the DTM was filled by taking the maximum of the two estimated surfaces at each point in the excised area. The result is a reasonable estimate of the original topography, at least near the DTM center, although there are small seams at the intersections and other minor discordant features. Flux estimates are given in Table 3. Estimates from these profiles range from $3 - 11 \times 10^6$ m^3 s^{-1}. Velocities in this reach were remarkably high, potentially exceeding 40 m s^{-1}. The fluxes calculated for the different cross-sections vary by a factor of ~2 for a given flow density and viscosity.

The lava surface morphology is illustrated in Fig. 6, in comparison with the more recent Athabasca Valles lava. The surface consists of a mix of rubbly, high-standing crust, which in some locations occurs in distinct plates. The relief of the plates in SKV appears greater than typical of the Athabasca Valles lava, suggesting a thicker breccia crust. Detached plates within the flow were mobile, while in other cases the crust was stationary, at least during the last stages of movement. (It is important to note that the preserved lava flow surface textures are not necessarily those that existed at peak flux.) Unfortunately, fine-scale morphologies in Kasei Valles are often obscured by blanketing dust. The plates in SKV typically appear as clusters of bouldery mounds separated by dust-filled lows, similar to lava flows in Daedalia Planum (Keszthelyi et al., 2008), while the fine-scale texture between the plates is occasionally dominated by ridges and hummocks of dust.

The geomorphology in this reach also yields some insights into lava erosion. Immediately upstream from the headwall, the channel rim elevation is quite close to the predicted original surface. Our estimated surface actually falls just below the rim level (Fig. 5), supporting the validity of the estimate. Therefore, erosion upstream from the inner channel appears to have been somewhere between small and non-existent. Because the flux estimates at D–D′ are the lowest of the three, D–D′ was probably not eroded after peak flux and might actually reflect aggradation due to incomplete drainage of the lava within the channel. Where the flow fills the second large hollow on the north bank, the high-lava mark is approximately 40 m below the top of the south bank. Barring unusual flow dynamics, there was a channel >40 m deep before emplacement of the SKV flow. Although this is a factor of several less than the final channel depth, the channel resembles cataracts or amphitheater-headed canyons formed by plunge-pool erosion and headwall retreat in large aqueous floods (e.g., Lamb et al., 2006, 2007, 2008). If it was largely cut by headward erosion processes (by either water or lava), at least half of the channel predated the lava flow. In this case erosion might have only been significant at the retreating cataract, consistent with the lack of erosion just upstream. This scenario is consistent with evidence for 1–2 km of cataract retreat at the upper cataract. Finally, the lava was entirely confined to the inner channel in places, so if it cut the channel, the flux would have had to rise very slowly from an initially low value so as to not overtop the banks at any time.

Between constriction 4 and the final DTM at the lower cataract, the flow is confined to the floor of a relatively straight valley. The flow width varies from ~5–20 km, but there are no distinctively eroded constrictions or topographic interactions like those upstream. Fig. 7 shows a typical example of this stretch, with a cross-section demonstrating that the net effect of the lava was to infill the channel. No flux calculations were made here; unlike B–B′ and C–C′, no information is available to check the reasonableness of interpolation from the walls, because the lava did not drain away. Hence such a calculation would necessarily be a rough approximation. For a 10-km-wide channel with a slope of 0.03° (typical values for the flow in SKV), the lower viscosities and hydraulic radii of 30–100 m give fluxes of $0.7–11 \times 10^6$ m^3 s^{-1} and velocities of 3.5–10.9 m s^{-1}. However, if the viscosity was 1000 Pa s and the flow much less than 100 m deep, the typical flow below the last

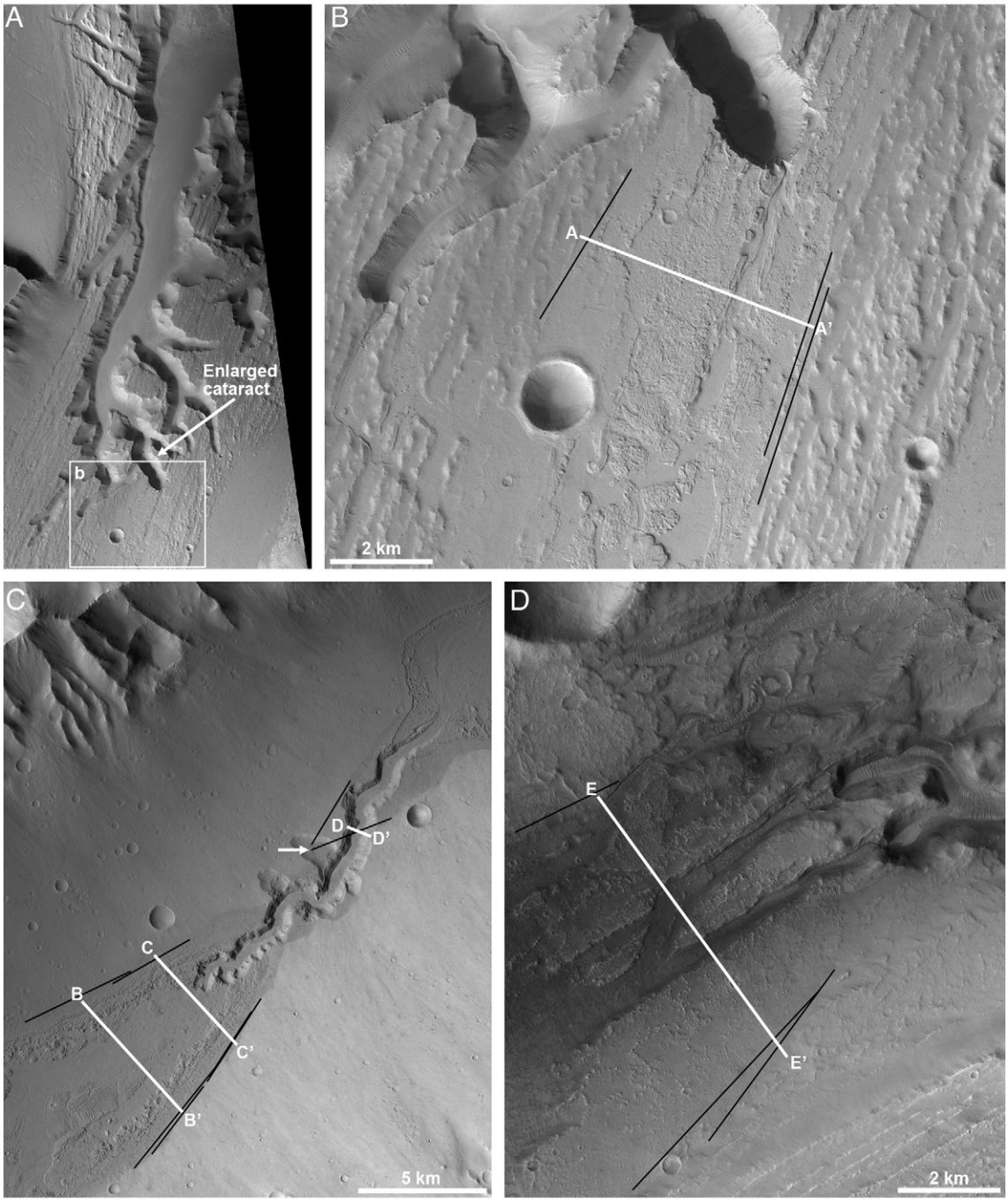

Fig. 2. Locations of cross-sectional profiles and slope measurements for flux modeling. A) Overview of the upper cataract. Note that the arm of the cataract that captured the lava flow is wider, deeper and more sharply defined than the other arms of the cataract, suggesting that the lava performed some erosion. B) Detail of lava entering the cataract. At some time lava continued past the main entry point and reached the next drainage, suggesting headward erosion of the main lava falls by the SKV flow. C) Locations of channel cross-sections near constriction 3. Arrow indicates a high-lava mark within a hollow that lies ~40 m below the opposite bank. D) Location of cross-section above lower cataract. For all cross-sections, black lines indicate locations of elevation offset measurements for slope calculations. The horizontal distance was determined by measuring the along-flow length of the black lines. For D–D′, the south bank was not used for upstream slope estimates because on the north bank the surface apparently drops steeply just upstream from our measurements. All images in this paper have been stretched to best show surface detail. Original images are available via the Planetary Data System. (A–B: CTX image B09_013297_1984_XN_18N074W. C: P03_002287_2005_XI_20N072W. D: P05_002814_2051_XI_25N061W. Images credit NASA/Jet Propulsion Laboratory (JPL)/Malin Space Science Systems (MSSS).).

constriction could have been laminar with much lower velocities and fluxes.

The fourth DTM (Fig. 2D) covers the head of the lower cataract, where we examine cross-section E–E′. Here the flow subdivides into three channels that carry the bulk of the flow and dominate the cross-sectional area. Flux estimates and flow parameters from this location are modestly greater than those from A–A′ (Table 3). We do not observe unambiguous evidence for or against lava erosion here. The incised channels above the lip of the falls could have been cut by lava but could also have been the result of earlier erosion. Since the setting and flux were similar to that just above the upper cataract, it is reasonable to expect that the erosive effects were similar, but this is unproven.

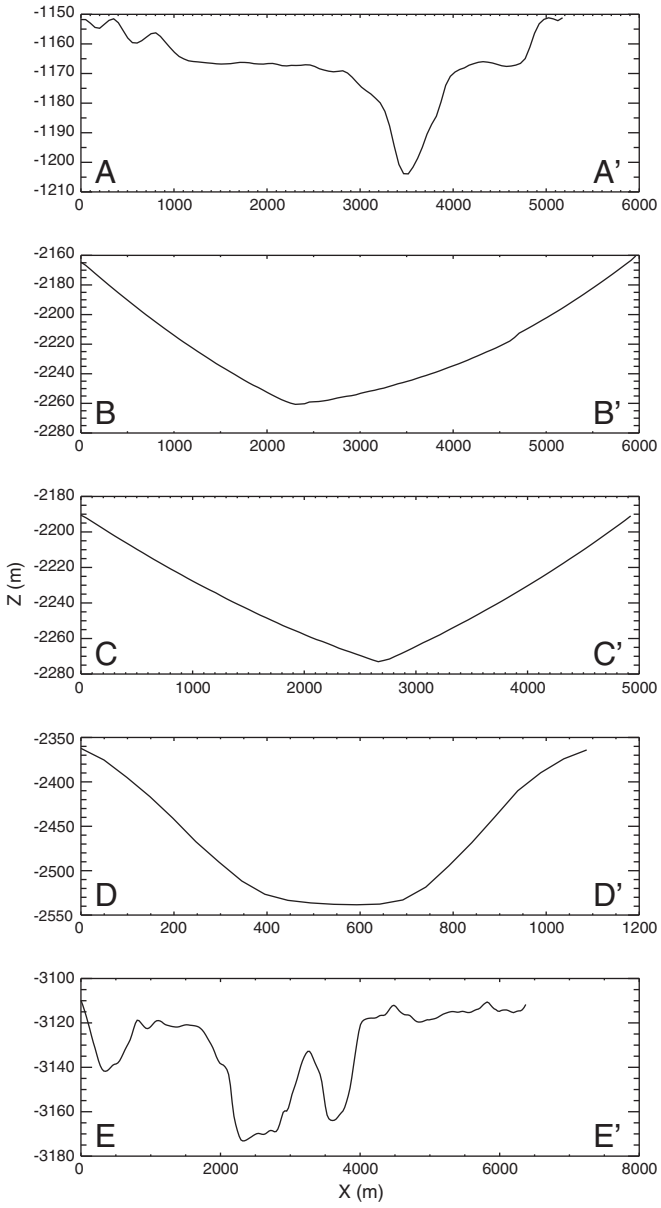

Fig. 3. Topographic profiles for cross-sections A–A′, B–B′, C–C′, D–D′, and E–E′. A, D and E use CTX DTM data. B and C use an estimated original surface described in the text.

One notable difference from the upper cataract is that the volume of lava that flowed past this point is less, which would reduce erosion.

4. Discussion

4.1. Emplacement dynamics

Lava in SKV was locally turbulent and records a very high peak flow rate. We estimate a peak lava flux of at least ~10^6 m^3 s^{-1}, which is 2–3 orders of magnitude greater than typical mean effusion rates for terrestrial flood lavas. Apparent variations along-flow are discussed below. We find very high velocities (>20 m s^{-1}) in some cases, but these only apply to the localized flow through steep, narrow constrictions. The SKV lava behaved in a manner similar to the Athabasca Valles flow. The Athabasca lava extended approximately 1400 km from its vent, matching our lower bound for SKV. In Athabasca Valles, Jaeger et al. (2010) estimated a lava flux of 5–20 × 10^6 m^3 s^{-1}, velocities of 5–10 m s^{-1}, and an eruption duration of days to weeks. Hence, the peak flux in SKV may have been modestly less vigorous. However, the estimates for Athabasca were made within 100 km of the vent and thus probably correspond well to the peak effusion rate, while peak fluxes at more distal points in SKV are likely to be less than the vent flux due to branching and attenuation. Like the Athabasca flow, the SKV lava was unambiguously turbulent in certain reaches for all reasonable rheological parameters, and almost certainly turbulent along much of its length if the viscosity was 100 Pa s or less.

Table 2
Measured parameters for flow modeling.

Cross-section	Cross-sectional area (m^2)	Hydraulic radius[a] (m)	Slope[b]
A–A′	87,000	17	0.33°
			0.22°
			0.26°
			Mean 0.27°
B–B′	370,000	61	0.28°
			0.35°
			0.30°
			Mean 0.31°
C–C′	220,000	46	0.77°
			0.71°
			0.71°
			Mean 0.72°
D–D′	120,000	99	0.32° [c]
			0.47° [c]
			Mean 0.39°
E–E′	140,000	22	0.20° [d]
			0.23° [d]
			0.49° [d]
			Mean 0.31°

[a] Calculated as cross-sectional area divided by wetted perimeter.
[b] Means taken on un-rounded values and then rounded.
[c] The south bank was not used for upstream slope estimates because on the north bank the surface apparently dropped steeply just upstream from our measurements, and south-bank lava is only found outside the channel further upstream.
[d] This scatter reflects differences between north and south bank values. Since there are several sub-channels within the flow draining into separate arms of the cataract, use of a single value is only a rough approximation.

Comparison of the flux estimates at different points along the flow produces some intriguing results. Regardless of the rheological parameters used, there is a mismatch between the flux estimates along-flow. The fluxes at cross-sections A–A′ and E–E′ differ by a factor of ~2, which may be due to the uncertainties in the slope measurement and possible variations in the flow properties (e.g., increase in viscosity) over hundreds of kilometers, and/or by erosion at E–E′ after the high-lava mark was established. Moreover, cross-section E–E′ spans three separate channels, which may affect the accuracy of the results and the appropriateness of a single slope value and simple hydraulic radius. However, the flux in the middle cross-sections is markedly higher than at either A–A′ or E–E′. This could be due to several factors. The low-viscosity cases have Reynolds numbers high enough that the application of Eq. (2) is questionable. Other possible factors are errors in measurement of the lava surface slope, which might have changed over short distances in the narrow confines of the channel, or differences between the cross-sectional profiles we used and the true substrate profile, for instance due to incomplete drainage at D–D′. Some combination of these effects must account for the variations between B–B′/C–C′ (which agree to within ~20%) and D–D′.

However, the very large increase in estimated peak flux between A–A′ and B–B′ may be a real effect. The high-lava mark in the basin between the upper cataract and constriction 1 is nearly level over tens of kilometers, and there is a cataract (Fig. 4) where the channel passes through the constriction. Headwall retreat at this cataract could have breached a pond and led to a sudden release of stored lava, temporarily producing a very high flux. By contrast, the high-lava mark upstream from constriction 3 is sloped and thus was probably established by actively flowing lava. The closer agreement between A–A′ and E–E′ supports the idea that these reflect the typical flow state, so it

Table 3
Modeled lava fluxes at cross-sections.

Profile	ρ (kg m^{-3})	η (Pa s)	Re[a]	<v> (m/s)[a]	Flux (10^6 m^3/s)[a]
A–A′	1400	10	26,000	11	0.95
	2300	10	45,000	12	1.0
	2900	10	58,000	12	1.0
	1400	100	1900	8.0	0.69
	2300	100	3300	8.6	0.74
	2900	100	4300	8.9	0.77
	1400	1000	54[c]	2.3	0.20
	2300	1000	140[c]	3.8	0.33
	2900	1000	230[c]	4.7	0.41
B–B′	1400	10	240,000[b]	28[b]	10[b]
	2300	10	410,000[b]	29[b]	11[b]
	2900	10	530,000[b]	30[b]	11[b]
	1400	100	19,000	22	7.9
	2300	100	32,000	23	8.4
	2900	100	42,000	24	8.6
	1400	1000	1300	16	5.7
	2300	1000	2400	17	6.1
	2900	1000	3100	17	6.4
C–C′	1400	10	240,000[b]	37[b]	8.3[b]
	2300	10	410,000[b]	39[b]	8.7[b]
	2900	10	520,00	40[b]	8.9[b]
	1400	100	18,000	29	6.4
	2300	100	32,000	30	6.8
	2900	100	41,000	31	7.0
	1400	1000	1300	21	4.6
	2300	1000	2300	22	5.0
	2900	1000	3000	23	5.2
D–D′	1400	10	610,000[b]	44[b]	5.0[b]
	2300	10	1,000,000[b]	45[b]	5.2[b]
	2900	10	1,300,000[b]	46[b]	5.3[b]
	1400	100	48,000	34	4.0
	2300	100	83,000	36	4.2
	2900	100	110,000[b]	37[b]	4.3[b]
	1400	1000	3500	25	2.9
	2300	1000	6200	27	3.1
	2900	1000	8100	28	3.2
E–E′	1400	10	42,000	14	1.9
	2300	10	74,000	15	2.0
	2900	10	95,000	15	2.1
	1400	100	3100	10	1.4
	2300	100	5500	11	1.5
	2900	100	7200	11	1.6
	1400	1000	130[c]	4.3	0.6
	2300	1000	350[c]	7.1	1.0
	2900	1000	520	8.3	1.1

[a] The number of decimal places shown does not reflect a detailed analysis of the measurement errors. See main text for discussion.
[b] For $Re > 10^5$ the equations in Section 2 may be inappropriate, but the inference of fast turbulent flow is unaffected. For $Re < 500$ the flow is laminar. In reality these transitions are not instantaneous.
[c] Laminar flow.

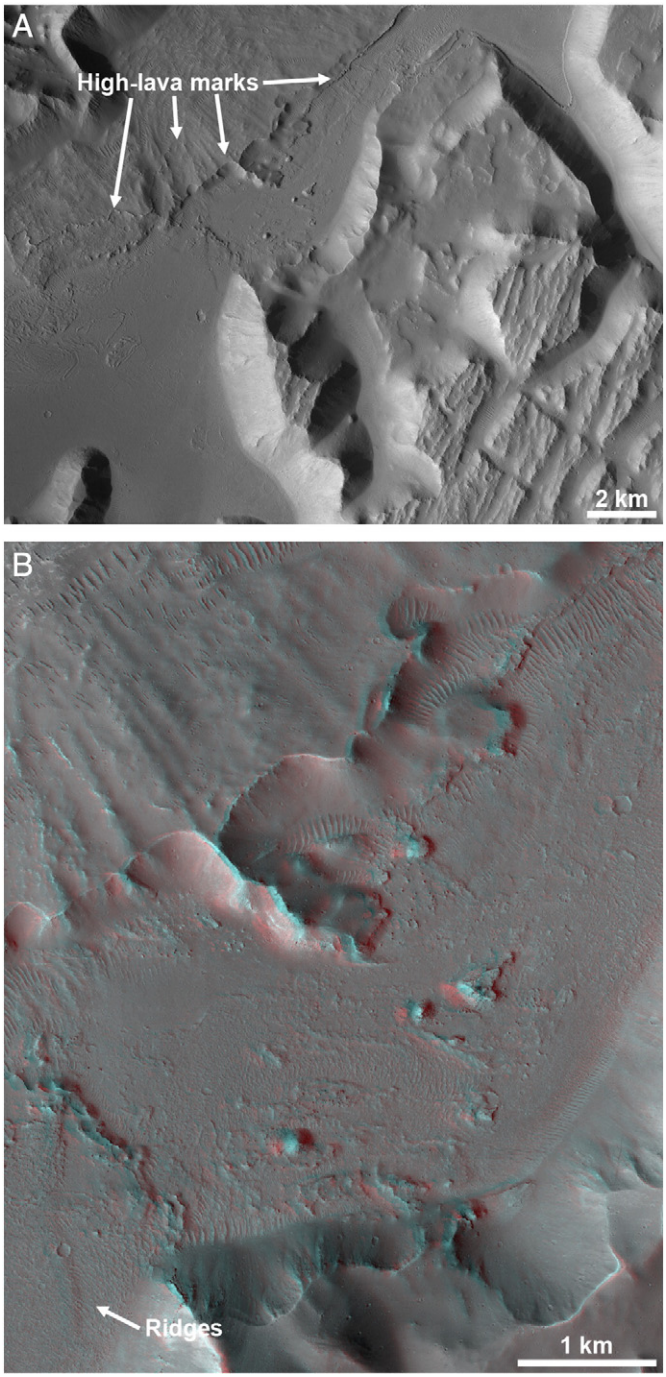

Fig. 4. A) Context view of constriction 1 and associated small cataract. The high-lava mark is indicated. Flow was to the upper right. (CTX image B05_011596_1992_XI_19N073W, credit NASA/JPL/MSSS.) B) Anaglyph of the cataract. There is no evidence of lava outside the channel more than a short distance downstream of the spur ridge at image center, so it is likely that the constricting channel existed below this point prior to emplacement of the lava flow, although the banks may have been undercut. Ridges at lower left are irregular and cratered and interpreted as lava flow surface structure. The ridges continue across the subtle scarp, so the scarp is not a lava flow front. (Anaglyph from HiRISE images ESP_031837_1990 and ESP_032193_1990, credit NASA/JPL/University of Arizona.).

is plausible that the high intermediate fluxes reflect a pulse of lava resulting from breaching a pond, which was attenuated before reaching the flow front or occurred before the flow had reached the lower cataract.

We therefore have the following scenario for the SKV lava flow. The bulk of the lava was emplaced with a maximum local flux on the order of 10^6 m^3 s^{-1}, as indicated by measurements at both the upper and lower cataracts. Since this is an estimate of the peak flux, the average over the entire history of the flow would have been lower. In terrestrial examples, the average flux is 2–10 times less than the peak (e.g., Wadge, 1981; Thordarson and Self, 1993). Locally higher flux estimates may have been the result of breaching the dam of a lava pond. Even the lower fluxes were capable of eroding headward at cataracts, as at A–A′. Headward erosion at lava falls has been previously reported (e.g., Greeley et al., 1998) so this is unsurprising, although the scale in SKVis considerably larger than terrestrial examples. Only in the highest-viscosity case would the peak flow have been (barely) laminar. The occurrence of a substantial crust favors scenarios that were not extremely turbulent, but this may not reflect the state of the flow at peak local flux.

We noted above that there are some candidate flow fronts within the SKV lava near the lower cataract. Although the similar preservation state suggests that they are due to late breakouts from the flow core rather than separate eruptions, detailed mapping will be needed to

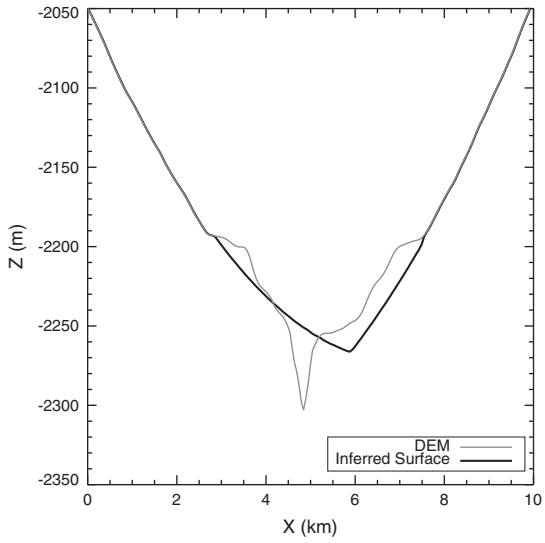

Fig. 5. Topographic profiles at the head of constriction 3 (just downstream from C–C′). The gray curve shows the current topography, including the incised channel, and the black curve shows the approximate pre-channel surface. Small kinks mark the boundary of the estimated surface. The lava had a net constructional effect on the flanks. At the channel center, the original surface was at approximately the same elevation as the rim of the inner channel. This suggests that there was little erosion upstream of the channel, since this agreement would not be expected if the near-level surface had also been significantly eroded.

fully understand the history of flows in Kasei Valles. Uncertainty from this question has no effect on the conclusions of this paper. The morphological assessments of erosion are purely local, as are the calculations of flux at specific cross-sections. Comparison of fluxes along the flow would seem to be compromised, but we are confident that the high-lava marks at A–D are from the same flow. Even if the flux calculated at E–E′ is from an earlier flow, the lava must have passed through A–A′ and the flux can have been no larger than was observed there, and all else being equal it is likely that the highest-flux eruption produced the longest flow. Hence, comparison of fluxes at A–A′ and E–E′ is still reasonable.

4.2. Erosive effects of large turbulent eruptions

Several cataracts were modified significantly by erosion by the SKV lava flow. However, the net effect on topography just upstream from constriction 3 was aggradational, and this is the case on the lower slopes of the typical channel further downstream as well. If basal erosion occurred, the topographic effect was nullified by lava emplacement. Therefore, lavas similar to the SKV flow do not appear responsible for the bulk incision of major outflow channels on Mars. Although the erosion of the upper cataract by the SKV flow was substantial, it nevertheless had a trivial effect on the gross plan-view shape and occupied only a small fraction of the grooved, eroded surface (Fig. 2A), so the fluid flux associated with carving that cataract must have been far larger. If lava eroded the major outflow channels, it must have erupted with much greater fluxes and/or longer flow durations than in SKV—yet of all well-described eruptions in the Solar System the peak flux of this flow is second only to the Athabasca Valles lava.

The Athabasca Valles lava had an even higher modeled peak flux, and it is likely that there was some amount of thermal (Cataldo et al., 2014) and mechanical (Keszthelyi et al., 2014) erosion in Athabasca Valles. Moreover, because Athabasca Valles is adjacent to the lava vent, the total volume of lava to flow past a given point was higher than for distal lava in SKV. However, most of the evidence for erosive processes in SKV is in the form of headwall recession at cataracts. Small cataracts are found within Athabasca Valles (e.g., Keszthelyi et al., 2007), but there is no evidence that the valley as a whole formed by cataract erosion. It is tempting to suggest that the greater flux of the Athabasca flow allowed it to cut that smaller channel, but there is a circularity problem in that the high flux estimate is dependent on the use of the final surface for topographic measurements. If the lava eroded the channel, the flux must have been lower than calculated by Jaeger et al. (2010) while the channel was first being incised, and never rose high enough to spill significantly outside the channel as it was eroding. Moreover, Athabasca Valles has many small distributaries that would have had to be eroded by considerably smaller lava fluxes, and traces of a buried crater rim on the floor of the main channel imply that at least part of the channel existed prior to the eruption (Dundas and Keszthelyi, 2013). Hence, while we expect that the Athabasca Valles lava had some erosive effects, there is reason to doubt that it was solely responsible for incising the channel.

4.3. Mechanical erosion rates

It appears that there was significant local retreat at cataract headwalls in Kasei Valles, but a relatively small amount of erosion in other reaches. Because of the high peak flux, lava erosion in SKV was likely by mechanical rather than thermal processes (c.f. Cataldo et al., 2014). Mechanical erosion rates of 0.1 m/day driven by entrained fragments within lava tubes have been reported (Kauahikaua et al., 1998), but they also noted that the rate can vary depending on the supply of debris falling from the roof and walls. These parameters may be significantly different in other settings, so we consider theoretical models. Siewert and Ferlito (2008) suggest that the mechanical erosion rate for lava undergoing abrasion is given by:

$$V_{mech} = k\rho g\left(\frac{Q}{W}\right)\cos(\theta)/H \tag{6}$$

where k is an empirically-determined proportionality constant (given as 10^{-3}–10^{-2} but with a broader possible range of 10^{-7}–10^{-1}; we take 10^{-3} as nominal), ρ is the lava density, g is the acceleration due to gravity, Q/W is the lava flux per unit width, θ is the slope, and H is the hardness (approximated as one-third of the yield strength, which is ~10^7 Pa for intact basalt). Note that abrasion in this model is by dragging or scraping particles rather than impacting entrained material, as commonly occurs in fluvial erosion. Hurwitz et al. (2010) suggest an alternate formulation based on stream-power or shear-stress erosion models used to study river erosion:

$$V_{mech} = K\rho g\left(\frac{Q}{W}\right)\sin(\theta) \tag{7}$$

where K is a different empirical proportionality constant (given as 10^{-9} Pa^{-1}, with a range of 10^{-10}–10^{-4}). The difference between the two is the use of bed shear stress vs. vertical load as the key erosive factor. For the reach just upstream of the first cataract (cross-section A–A′, where there is evidence for erosion by a process other than cataract retreat) and the nominal values of the proportionality constants, Eqs. (6) and (7) predict peak erosion rates of 27 m/day and 0.5 m/day, respectively. The inner channel there is tens of meters deep (Fig. 3A), so erosion rates peaking in this range are consistent with a short eruption.

Unfortunately, these estimates differ by nearly two orders of magnitude. Due to the empirical and situation-dependent nature of the proportionality constants there is substantial uncertainty in these rates—it would be equally justified to infer erosion rates from estimates for the flow duration and use those to determine the constants for each model, but this limits the predictive value of the models. Indeed, the value for K preferred by Hurwitz et al. (2010) was based on giving the "most reasonable results" given other constraints on the lava they examined, a small flow down a steep talus slope, and a value fives times higher was used for bedrock erosion in other work (Hurwitz et al.,

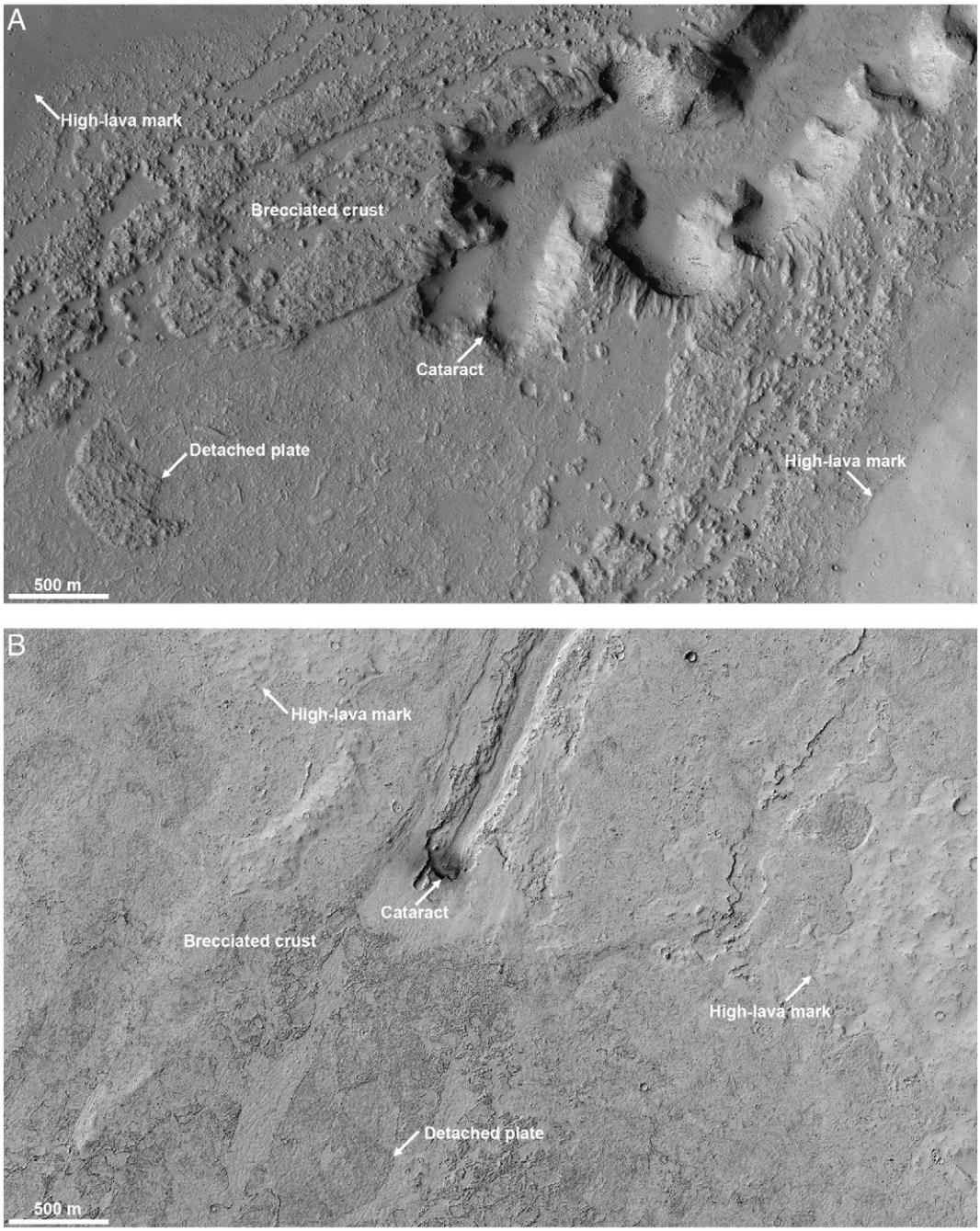

Fig. 6. Comparison of lava in similar settings in Kasei Valles (A) and the Athabasca Valles lava flow (B). Both locations exhibit brecciated crusts that have broken into detached plates in places. Flow is towards the upper right in both panels. The relief of the platy surface in Kasei Valles is greater, suggesting a thicker brecciated crust. (A: HiRISE image PSP_002287_2010. B: PSP_008990_1860. Images credit NASA/JPL/University of Arizona.).

2013a). This is surprising, as bedrock should be more resistant to erosion than loose talus. The value of k from Siewert and Ferlito (2008) was empirically estimated from a single flow in Sicily, which was not turbulent and may give an atypically high erosion rate since the substrate was warm, soft lava. It is not clear that the same values apply to Kasei Valles, with potentially different substrate lithology and competence as well as flow crystallinity and abundance of entrained particles.

We suggest that models for mechanical lava erosion like Eqs. (6) and (7) should be treated with caution until the physical processes are better understood. Note that both equations imply that all lavas are erosive, which is not the case. Additionally, there is ongoing debate over the controls on the far better-studied problem of fluvial erosion. For instance, Johnson and Whipple (2010) suggest that bedrock erosion has no direct dependence on shear stress, but rather depends on parameters that correlate with shear stress in natural fluvial channels. It is not clear how similar those correlations would be in a lava flow. Major fluvial erosive processes include plucking of jointed rock, abrasion by entrained particles, and cavitation, where bubbles in the flow collapse (e.g., Whipple et al., 2000). These processes have different exponential dependences on the shear stress or stream power. (Eq. (7) implicitly uses plucking.) Plucking bedrock involves flow through thin joints around a block (Whipple et al., 2000). A plucking-like process may be a reasonable description for the talus slope erosion studied by Hurwitz et al. (2010) or for protruding blocks, but through-flow around blocks of massive jointed bedrock is improbable. Unlike terrestrial rivers,

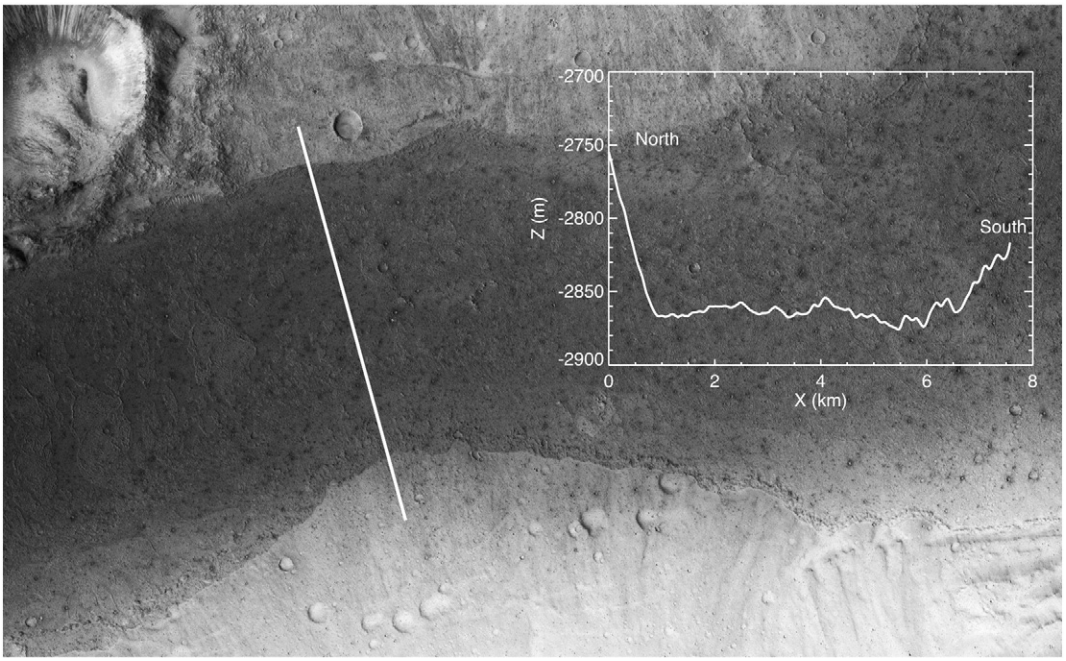

Fig. 7. Typical segment of Kasei Valles. In locations that are not immediately upstream from steep channel reaches where the lava drained, the channel floor has been infilled and is nearly flat, apart from roughness on the lava flow surface. Some erosion of the substrate may have occurred, but the overall effect of the lava was clearly to build up the surface. (CTX image G15_024215_2048_XN_24N069W, credit NASA/JPL/MSSS.).

most lava is bubble-rich under typical flow conditions, so bubbles probably do not collapse due to normal variations in the flow. Abrasion may occur when there is no chilled crust at the base of a lava flow, but abrasive particles must first be supplied and there is no reason to assume that the relationship between shear stress and particle abrasion will be the same for lava and water. Small, hot grains or crystals in a lava flow will be soft and less effective at abrading bedrock, and the amount of entrained solid material could be quite variable. Therefore, scaling fluvial erosion laws to lava is not straightforward when the details of physical processes are considered. Given the uncertain empirical constants, we consider sufficiently low rates of mechanical erosion away from the cataracts in SKV to be plausible.

5. Conclusions

The south Kasei Valles lava represents the second example of a large, turbulent, platy-ridged flood lava on Mars. In scale and eruption style, this lava resembles the well-documented flow in Athabasca Valles. Although both inflated flows and lava tubes have been confirmed on Mars, this turbulent eruption style may be a common emplacement process for at least the most recent large flood lavas, in contrast with terrestrial flood lavas.

Observations of lava in south Kasei Valles place constraints on the erosive effectiveness of such massive flows. The lava eroded headwards at steep cataracts, but the scale of erosion in Kasei Valles and other Martian outflow channels is far greater than the inferred erosion by this flow. In other reaches, probably along most of its length, the net effect of the flow was aggradational even if some basal erosion occurred. Therefore, flows like the SKV lava were not responsible for carving the major Martian outflow channels, although SKV records one of the largest and most vigorous well-preserved effusive eruptions in the Solar System. This supports the interpretation that the main erosive process responsible for the outflow channels was large water floods, unless far larger and more erosive volcanic eruptions were common in the past. However, smaller channels and significant local erosion can occur due to lava.

Acknowledgments

We thank the HiRISE and CTX operations teams for their work in acquiring the images used in this study, and Donna Galuszka, Bonnie Redding and Eric Foster for producing the DTMs. Ken Tanaka and Justin Hagerty gave helpful comments on an early draft, and Jacob Bleacher and Christopher Hamilton provided thoughtful reviews. This work was supported by NASA Mars Data Analysis Program grant NNH08AI66I, Planetary Geology and Geophysics Program grant NNX12AR66G and the Mars Reconnaissance Orbiter HiRISE project.

References

Alberti, G., Castaldo, L., Orosei, R., Frigeri, A., Cirillo, G., 2012. Permittivity estimates over Mars by using SHARAD data: the Cerberus Palus area. J. Geophys. Res. 117. http://dx.doi.org/10.1029/2012JE004047.

Baker, V.R., 1982. The Channels of Mars. University of Texas Press, Austin, (198 pp.).

Baker, V.R., Komatsu, G., Parker, T.J., Gulick, V.C., Kargel, J.S., Lewis, J.S., 1992. Channels and valleys on Venus: preliminary analysis of Magellan data. J. Geophys. Res. 97, 13,421–13,444.

Bird, R.B., Stewart, W.E., Lightfoot, E.N., 1960. Transport Phenomena. John Wiley, New York, (780 pp.).

Carr, M.H., 1974. The role of lava erosion in the formation of lunar rilles and Martian channels. Icarus 22, 1–23.

Cataldo, V., Williams, D.A., Dundas, C., Keszthelyi, L., 2014. Athabasca Valles, Mars: how important was erosion by lava? Lunar Planet. Sci. Conf. 45 (abstract #1154).

Caudill, C.M., Tornabene, L.L., McEwen, A.S., Byrne, S., Ojha, L., Mattson, S., 2012. Layered megablocks in the central uplifts of impact craters. Icarus 221, 710–720.

Chapman, M.G., Neukum, G., Dumke, A., Michael, G., van Gasselt, S., Kneissl, T., Zuschneid, W., Hauber, E., Mangold, N., 2010. Amazonian geologic history of the Echus Chasma and Kasei Valles system on Mars: new data and interpretations. Earth Planet. Sci. Lett. 294, 238–255.

Christensen, P.R., Jakosky, B.M., Kieffer, H.H., Malin, M.C., McSween, H.Y., Nealson, K., Mehall, G.L., Silverman, S.H., Ferry, S., Caplinger, M., Ravine, M., 2004. The Thermal Emission Imaging System (THEMIS) for the Mars 2001 Odyssey Mission. Space Sci. Rev. 110, 85–130.

Dundas, C.M., Keszthelyi, L.P., 2013. Modeling steam pressure under Martian lava flows. Icarus 226, 1058–1067.

Goncharov, V.N., 1964. Dynamics of channel flow. Translated from Russian by Israel Program Science TranslationUS Department of Commerce, Office of Technical Services, Washington, D. C, (317 pp.).

Greeley, R., Schneid, B.D., 1991. Magma generation on Mars: amounts, rates, and comparisons with Earth, Moon, and Venus. Science 254, 996–998.

Greeley, R., Fagents, S.A., Harris, R.S., Kadel, S.D., Williams, D.A., Guest, J.E., 1998. Erosion by flowing lava: field evidence. J. Geophys. Res. 103, 27,325–27,345.
Harris, A.J.L., Dehn, J., Calvari, S., 2007. Lava effusion rate definition and measurement: a review. Bull. Volcanol. 70, 1–22.
Head, J.W., Chapman, C.R., Strom, R.G., Fassett, C.I., Denevi, B.W., Blewett, D.T., Ernst, C.M., Watters, T.R., Solomon, S.C., Murchie, S.L., Prockter, L.M., Chabot, N.L., Gillis-Davis, J.J., Whitten, J.L., Goudge, T.A., Baker, D.M.H., Hurwitz, D.M., Ostrach, L.R., Xiao, Z., Merline, W.J., Kerber, L., Dickson, J.L., Oberst, J., Byrne, P.K., Klimczak, C., Nittler, L.R., 2011. Flood volcanism in the northern high latitudes of Mercury revealed by MESSENGER. Science 333, 1853–1856.
Hurwitz, D.M., Head, J.W., 2012. Testing the late-stage outflow channel origin hypothesis: investigating both water erosion and lava erosion origins for Athabasca Valles, Mars. Lunar Planet. Sci. Conf. 43 (abstract #1056).
Hurwitz, D.M., Fassett, C.I., Head, J.W., Wilson, L., 2010. Formation of an eroded lava channel within an Elysium Planitia impact crater: distinguishing between a mechanical and thermal origin. Icarus 210, 626–634.
Hurwitz, D.M., Head, J.W., Byrne, P.K., Xiao, Z., Solomon, S.C., Zuber, M.T., Smith, D.E., Neumann, G.A., 2013a. Investigating the origin of candidate lava channels on Mercury with MESSENGER data: theory and observations. J. Geophys. Res. 118. http://dx.doi.org/10.1029/2012JE004103.
Hurwitz, D.M., Head, J.W., Hiesinger, H., 2013b. Lunar sinuous rilles: distribution, characteristics, and implications for their origin. Planet. Space Sci. 79–80, 1–38.
Jaeger, W.L., Keszthelyi, L.P., McEwen, A.S., Dundas, C.M., Russell, P.S., 2007. Athabasca Valles, Mars: a lava-draped channel system. Science 317, 1709–1711.
Jaeger, W.L., Keszthelyi, L.P., Skinner, J.A., Milazzo, M.P., McEwen, A.S., Titus, T.N., Rosiek, M.R., Galuszka, D.M., Howington-Kraus, E., Kirk, R.L., The HiRISE Team, 2010. Emplacement of the youngest flood lava on Mars: a short, turbulent story. Icarus 205, 230–243.
Jeffreys, H., 1925. Flow of water in an inclined channel of rectangular section. Phil. Mag. J. Sci. 49, 793–807.
Johnson, J.P.L., Whipple, K.X., 2010. Evaluating the controls of shear stress, sediment supply, alluvial cover, and channel morphology on experimental bedrock incision rate. J. Geophys. Res. 115, F02018. http://dx.doi.org/10.1029/2009JF001335.
Kauahikaua, J., Cashman, K.V., Mattox, T.N., Heliker, C.C., Hon, K.A., Mangan, M.T., Thornber, C.R., 1998. Observations on basaltic lava streams in tubes from Kilauea Volcano, island of Hawai'i. J. Geophys. Res. 103 (B11), 27,303–27,323.
Keszthelyi, L., McEwen, A., 2007. Comparison of flood lavas on Earth and Mars. In: Chapman, M.G. (Ed.), The Geology of Mars. Cambridge University Press, New York.
Keszthelyi, L., Self, S., 1998. Some physical requirements for the emplacement of long basaltic lava flows. J. Geophys. Res. 103, 27,447–27,464.
Keszthelyi, L., McEwen, A.S., Thordarson, T., 2000. Terrestrial analogs and thermal models for Martian flood lavas. J. Geophys. Res. 105, 15,027–15,049.
Keszthelyi, L., Thordarson, T., McEwen, A., Haack, H., Guilbaud, M.-N., Self, S., Rossi, M.J., 2004. Icelandic analogs to Martian flood lavas. Geochem. Geophys. Geosyst. 5. http://dx.doi.org/10.1029/2004GC000758.
Keszthelyi, L., Self, S., Thordarson, T., 2006. Flood lavas on Earth, Io and Mars. J. Geol. Soc. London 163, 253–264.
Keszthelyi, L.P., Denlinger, R.P., O'Connell, D.R.H., Burr, D.M., 2007. Initial insights from 2.5D hydraulic modeling of floods in Athabasca Valles, Mars. Geophys. Res. Lett. 34, L21206. http://dx.doi.org/10.1029/2007GL031776.
Keszthelyi, L., Jaeger, W., McEwen, A., Tornabene, L., Beyer, R.A., Dundas, C., Milazzo, M., 2008. High Resolution Imaging Science Experiment (HiRISE) images of volcanic terrains from the first six months of the Mars Reconnaissance Orbiter Primary Science Phase. J. Geophys. Res. 113, E04005. http://dx.doi.org/10.1029/2007JE002968.
Keszthelyi, L., Jaeger, W., Dundas, C.M., Williams, D.A., Cataldo, V., 2014. Evidence for possible mechanical erosion by lava at Athabasca Valles, Mars from HiRISE and CTX images and topography. Lunar Planet. Sci. Conf. 45 (abstract #1683).
Kirk, R.L., Howington-Kraus, E., Rosiek, M.R., Anderson, J.A., Archinal, B.A., Becker, K.J., Cook, D.A., Galuszka, D.M., Geissler, P.E., Hare, T.M., Holmberg, I.M., Keszthelyi, L.P., Redding, B.L., Delamere, W.A., Gallagher, D., Chapel, J.D., Eliason, E.M., King, R., McEwen, A.S., 2008. Ultrahigh resolution topographic mapping of Mars with MRO HiRISE stereo images: meter-scale slopes of candidate Phoenix landing sites. J. Geophys. Res. 113. http://dx.doi.org/10.1029/2007JE003000.
Lamb, M.P., Howard, A.D., Johnson, J., Whipple, K.X., Dietrich, W.E., Perron, J.T., 2006. Can springs cut canyons into rock? J. Geophys. Res. 111. http://dx.doi.org/10.1029/2005JE002663.
Lamb, M.P., Howard, A.D., Dietrich, W.E., Perron, J.T., 2007. Formation of amphitheater-headed valleys by waterfall erosion after large-scale slumping on Hawai'i. Geol. Soc. Am. Bull. 119, 805–822.
Lamb, M.P., Dietrich, W.E., Aciego, S.M., DePaolo, D.J., Manga, M., 2008. Formation of Box Canyon, Idaho, by megaflood: implications for seepage erosion on Earth and Mars. Science 320, 1067–1070.
Leone, G., 2014. A network of lava tubes as the origin of Labyrinthus Noctis and Valles Marineris on Mars. J. Volcanol. Geotherm. Res. 277, 1–8.
Leverington, D.W., 2004. Volcanic rilles, streamlined islands, and the origin of outflow channels on Mars. J. Geophys. Res. 109, E10011. http://dx.doi.org/10.1029/2004JE002311.
Leverington, D.W., 2007. Was the Mangala Valles system incised by volcanic flows? J. Geophys. Res. 112, E11005. http://dx.doi.org/10.1029/2007JE002896.
Leverington, D.W., 2009. Reconciling channel formation mechanisms with the nature of elevated outflow systems at Ophir and Aurorae Plana, Mars. J. Geophys. Res. 114, E10005. http://dx.doi.org/10.1029/2009JE003398.
Leverington, D.W., 2011. A volcanic origin for the outflow channels of Mars: key evidence and major implications. Geomorphology 132, 51–75.
Malin, M.C., Bell, J.F., Cantor, B.A., Caplinger, M.A., Calvin, W.C., Clancy, R.T., Edgett, K.S., Edwards, L., Haberle, R.M., James, P.B., Lee, S.W., Ravine, M.A., Thomas, P.C., Wolff, M.J., 2007. Context Camera investigation on board the Mars Reconnaissance Orbiter. J. Geophys. Res. 112. http://dx.doi.org/10.1029/2006JE002808.
Mangold, N., Loizeau, D., Poulet, F., Ansan, V., Baratoux, D., Le Mouelic, S., Bardintzeff, J.M., Platevoet, B., Toplis, M., Pinet, P., Masson, P., Bibring, J.P., Gondet, B., Langevin, Y., Neukum, G., 2010. Mineralogy of recent volcanic plains in the Tharsis region, Mars, and implications for platy-ridged flow composition. Earth Planet. Sci. Lett. 294, 440–450.
McEwen, A.S., Malin, M.C., Carr, M.H., Hartmann, W.K., 1999. Voluminous volcanism on early Mars revealed in Valles Marineris. Nature 397, 584–586.
McSween, H.Y., Taylor, G.J., Wyatt, M.B., 2009. Elemental composition of the Martian crust. Science 324, 736–739.
Self, S., Thordarson, T., Keszthelyi, L., Walker, G.P.L., Hon, K., Murphy, M.T., Long, P., Finnemore, S., 1996. A new model for the emplacement of Columbia River basalts as large, inflated pahoehoe flows. Geophys. Res. Lett. 23, 2,689–2,692.
Self, S., Thordarson, T., Keszthelyi, L., 1997. Emplacement of continental flood basalt lava flows. In: Mahoney, J.J., Coffin, M.F. (Eds.), Large Igneous Provinces: Continental, Oceanic and Planetary Flood Volcanism. Geophysical Monograph, 100. American Geophysical Union.
Self, S., Keszthelyi, L., Thordarson, T., 1998. The importance of pahoehoe. Ann. Rev. Earth Planet. Sci. 26, 81–110.
Shaw, H.R., Swanson, D.A., 1970. Eruption and flow rates of flood basalts. In: Gilmour, E.H., Stradling, D.F. (Eds.), Proceedings of the Second Columbia River Basalt Symposium. Eastern Washington State College, Cheney, pp. 271–299.
Siewert, J., Ferlito, C., 2008. Mechanical erosion by flowing lava. Contemp. Phys. 49, 43–54.
Swanson, D.A., 1973. Pahoehoe flows from the 1969–1971 Mauna Ulu eruption, Kilauea Volcano, Hawaii. Geol. Soc. Am. Bull. 84, 615–626.
Swanson, D.A., Wright, T.L., Helz, R.J., 1975. Linear vent systems and estimated rates of magma production and eruption for the Yakima basalt on the Columbia River Plateau. Am. J. Sci. 275, 877–905.
Thordarson, T., Self, S., 1993. The Laki (Skaftár Fires) and Grímsvötn eruptions in 1783–1785. Bull. Volcanol. 55, 233–263.
Wadge, G., 1981. The variation of magma discharge during basaltic eruptions. J. Volcanol. Geotherm. Res. 11, 139–168.
Whipple, K.X., Hancock, G.S., Anderson, R.S., 2000. River incision into bedrock: mechanics and relative efficacy of plucking, abrasion, and cavitation. Geol. Soc. Am. Bull. 112, 490–503.
Williams, R.M.E., Malin, M.C., 2004. Evidence for late stage fluvial activity in Kasei Valles, Mars. J. Geophys. Res. 109. http://dx.doi.org/10.1029/2003JE002178.